
Better Battery Usage From the Insights of Modeling

Summary

In this paper, we develop a equivalent model to analyze and predict the performance of Li-Ion batteries in smartphones under various operating conditions.

We start by constructing a simplest reasonable model based on ideal battery assumptions, which provides a foundational understanding of battery behavior. An 2-order Thevenin model is build without considering temperature, power demand, smartphone heating and other factors. Then dataset from related HPPC tests are used to identify the model parameters. Because the differential equation can not be solved analytically, numerical methods are employed to validated the model, showing logical and intuitive results.

Next, we refine the model by incorporating real-world factors. The Arrhenius equation is introduced to account for temperature effects on battery performance. It is observed that the internal resistance increases exponentially with decreasing temperature, leading to higher voltage drops under load. We also consider the decomposition of smartphone power consumption, revealing that components like the data network and CPU significantly impact battery drain. With these results, we further analyze smartphones' self-heating effect during operation, which in turn affects battery temperature and performance. All of the results above should answer Question 1 and Question 2.

Then, a sensitivity analysis is conducted to identify the most influential parameters affecting battery life and performance. It has not escaped our eyes that *SOC*-dependent(so time-dependent) parameters, such as internal resistance and capacity, capture the suddenly degradation behavior of batteries at low *SOC* state. Simply setting those parameters as constants may lead to significant errors in long-term predictions. We also apply numerical distribution to parameters, quantifying the uncertainty in model outputs due to parameter variability in different scenarios. This part should answer Question 3.

Finally, based on the insights gained from our modeling and analysis, we provide practical recommendations for optimizing battery usage in smartphones. This part should answer Question 4.

Keywords: Smartphone; Li-Ion Battery; 2-Order Thevenin Model; Arrhenius Equation; Sensitivity Analysis

Contents

| | | |
|----------|--|-----------|
| 1 | Introduction | 3 |
| 1.1 | Problem Background | 3 |
| 1.2 | Restatement of the Problem | 3 |
| 1.3 | Our Work | 4 |
| 2 | Ideal Battery | 4 |
| 2.1 | Assumptions | 4 |
| 2.2 | Thevenin Model | 4 |
| 2.3 | Parameter Estimation | 6 |
| 2.4 | Simulations | 9 |
| 2.4.1 | Constant current | 9 |
| 2.4.2 | Constant power | 9 |
| 3 | Actual Battery | 10 |
| 3.1 | Assumptions | 10 |
| 3.2 | Temperature Behavior of Battery | 10 |
| 3.3 | Battery in Different Work Loads | 12 |
| 3.3.1 | Screen Power | 12 |
| 3.3.2 | CPU Power | 12 |
| 3.3.3 | Network Power | 13 |
| 3.3.4 | GPS Power | 13 |
| 3.3.5 | Audio Power | 13 |
| 3.3.6 | System Mode Power Adjustment | 14 |
| 3.3.7 | Parameter Estimation and Validation | 14 |
| 3.3.8 | Usage Scenario Simulation | 15 |
| 3.4 | Heat Transfer Model in High-Performance Scenarios | 16 |
| 4 | Sensitivity Analysis | 17 |
| 4.1 | Time-Varying Properties | 17 |
| 4.2 | Numerical Accuracy | 18 |
| 5 | User Recommendations | 19 |
| 5.1 | Short-Term Recommendations: Extending Battery Runtime | 19 |
| 5.2 | Long-Term Recommendations: Maximizing Battery Lifespan | 20 |
| A | Notation | 22 |
| B | References | 24 |
| C | Use of AI | 25 |
| C.1 | Battery Dataset Selection | 25 |
| C.2 | Dataset Overview and Statistics | 25 |
| C.3 | Coefficient Reasonableness Analysis | 26 |
| C.4 | Data Sampling Strategy | 26 |
| C.5 | LaTeX Equation Formatting | 27 |
| C.6 | LaTeX Table Column Width Adjustment | 27 |
| C.7 | Summary of AI Usage | 28 |
| C.8 | Declaration | 28 |

1 Introduction

1.1 Problem Background

Smartphone has become an indispensable part of our daily lives. What plays a key role in user experience and smartphones' design is the development of smartphone battery. From where consumers stand, we don't want to be anxious as battery's draining behaviour is affected by a tremendous amount of factors, like the processor load and the ambient temperature. Still, as manufacturers, we need to provide the most accurate prediction of the as a competitive edge, and most importantly, to adapt subsequent measures to increase battery's lifespan, which helps a lot in environmental sustainability. All of these are calling for more-detailed physical models and optimized algorithm predictions.



1.2 Restatement of the Problem

Based on the background, our aim is to establish an algorithm from the very physical essence of battery theory and user's data, through which we could finally help users to predict the time-to-empty under different circumstances and adapt adequate optimizations. So we need to address:

1. **Continuous-Time Model:** Deriving a set of differential equations from lithium battery's principle, establishing an ideal and then an actual model that returns the SOC as a function of time, and using collected data to validate and support them.
2. **Time-to-Empty Predictions:** Approximating the time-to-empty from different initial charge level, and introduce complex conditions to find the differences.
3. **Sensitivity Analysis:** Introducing fluctuations of usage patterns or making changes to some flexible parameters or the assumptions to examine the model for lithium batteries is solid.
4. **Recommendations:** Finding out optimization strategies of improving battery life, considering battery aging's impact on effective capacity's reduction, and trying to generalize to other portable devices.

1.3 Our Work

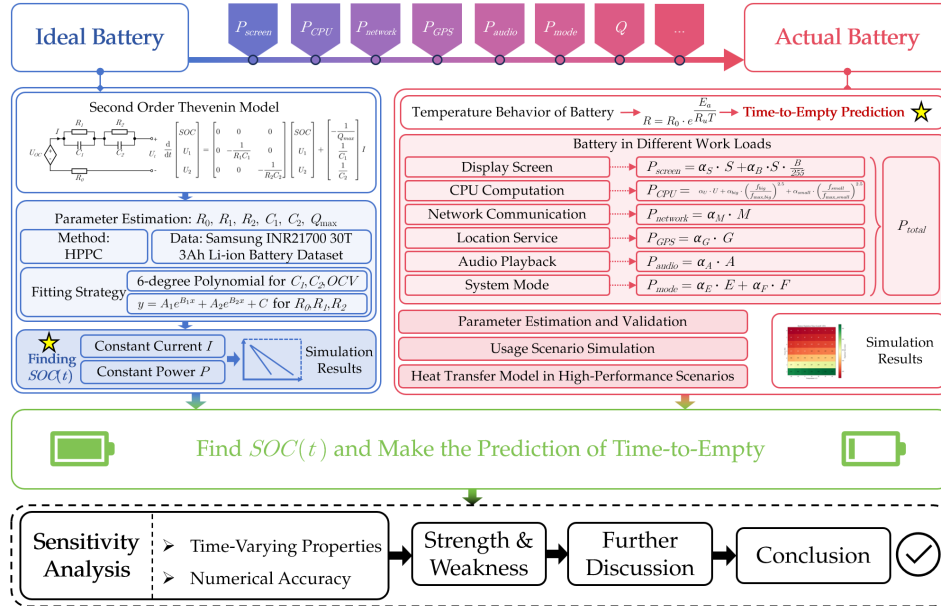


Figure 1: Flowchart of Our Work

2 Ideal Battery

2.1 Assumptions

To consider an simplest ideal battery model, the following assumptions are made:

- The battery is kept at a constant environment, so the temperature effects are neglected.
- The battery has no energy loss during charging and discharging.
- The battery has infinite cycle life, so the degradation effects are neglected and all the parameters are constant.
- The Open Circuit Voltage (OCV) is only related to the SOC , so we can express the SOC as a function of U_{OC} :

$$SOC = f(U_{OC}) \quad (1)$$

in which $f(\cdot)$ can be obtained through curve fitting based on experimental data.

- The battery behavior is same for charging and discharging. For smartphones, which mostly use LiCoO₂ batteries that has little or no hysteresis, this assumption is reasonable.

2.2 Thevenin Model

A Li-ion battery system can be extremely complex, involving electrochemical, thermal and mechanical processes. However, for system-level studies, an equivalent circuit model is often used to represent the battery behavior [2]. The 2-order Thevenin model is a widely used equivalent circuit model that captures the dynamic response of the battery voltage during charge and discharge cycles. The model is described as follows:

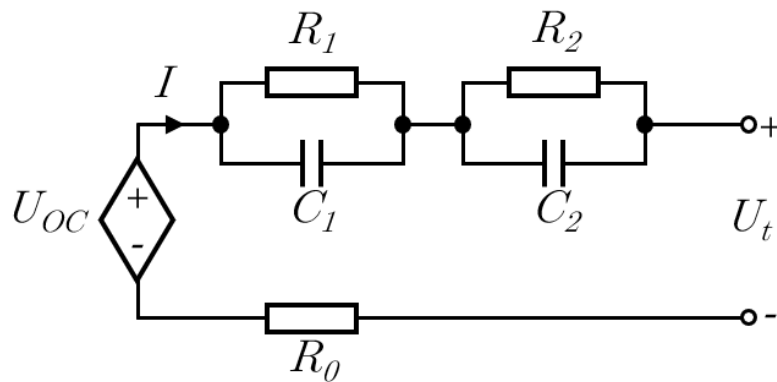


Figure 2: Thevenin Model Circuit

In electrochemistry, the polarization effects are often divided into two main categories: electrochemical polarization and concentration polarization. The former is caused by the charge transfer resistance at the electrode/electrolyte interface, while the latter is due to the mass transport limitations within the electrode materials. In the Thevenin model, these two polarization effects are represented by two RC networks: R_1, C_1 for electrochemical polarization and R_2, C_2 for concentration polarization.

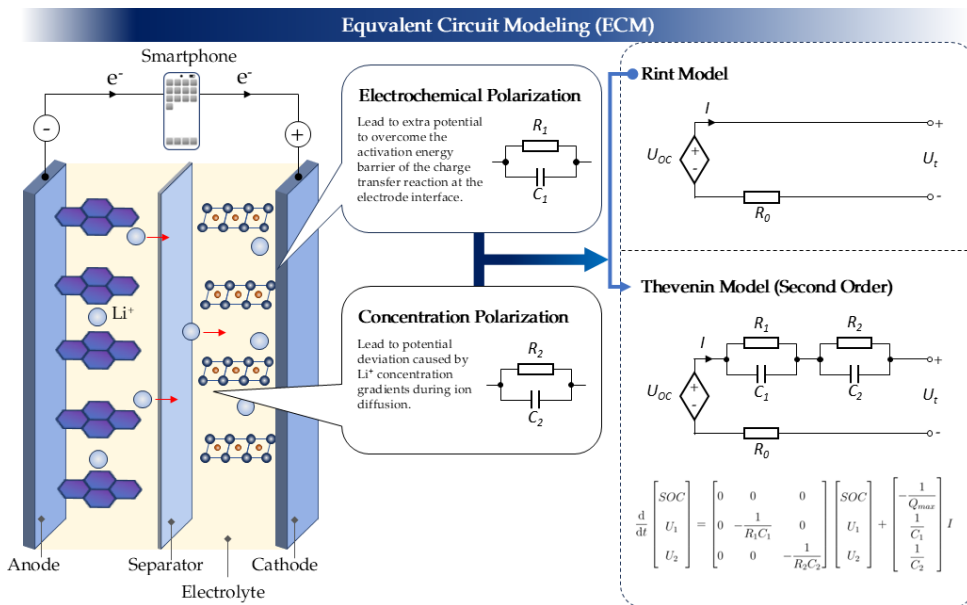


Figure 3: Battery and Its Model Equivalent Circuit

The relationship between U_{OC} and other parameters in the Thevenin model can be expressed with Kirchhoff's laws:

$$U_{OC} = U_t + IR_0 + U_1 + U_2 \quad (2)$$

in which U_t is the terminal voltage.

For U_1, U_2 we have:

$$I = C_1 \frac{dU_1}{dt} + \frac{U_1}{R_1} = C_2 \frac{dU_2}{dt} + \frac{U_2}{R_2} \quad (3)$$

Differentiateing the *SOC*'s definition with respect to time, we get:

$$\frac{d(SOC)}{dt} = -\frac{I}{Q_{max}} \quad (4)$$

where Q_{max} is the maximum capacity of the battery.

Combining the above equations, we can derive the complete Thevenin model in matrix form:

$$\frac{d}{dt} \begin{bmatrix} SOC \\ U_1 \\ U_2 \end{bmatrix} = \begin{bmatrix} 0 & 0 & 0 \\ 0 & -\frac{1}{R_1 C_1} & 0 \\ 0 & 0 & -\frac{1}{R_2 C_2} \end{bmatrix} \begin{bmatrix} SOC \\ U_1 \\ U_2 \end{bmatrix} + \begin{bmatrix} -\frac{1}{Q_{max}} \\ \frac{1}{C_1} \\ \frac{1}{C_2} \end{bmatrix} I \quad (5)$$

where $R_0, R_1, R_2, C_1, C_2, Q_{max}$ are the model parameters that need to be estimated.

However, if the battery is in an open-circuit state, the structure of the circuit will change:

In that case, since $I = 0$, there is no voltage drop across R_0 , so the terminal voltage U_t is expressed by:

$$U_t = U_{OC} - U_1 - U_2 \quad (6)$$

Both of the capacitors C_1, C_2 will slowly discharge through their respective resistors R_1, R_2 , expressed as:

$$\frac{dU_1}{dt} = -\frac{U_1}{R_1 C_1}, \quad \frac{dU_2}{dt} = -\frac{U_2}{R_2 C_2} \quad (7)$$

Combining (6) and (7), we can get the analytic solution:

$$U_t = U_{OC} - U_{1,init} e^{-\frac{t}{R_1 C_1}} - U_{2,init} e^{-\frac{t}{R_2 C_2}} \quad (8)$$

where $U_{1,init}, U_{2,init}$ are the initial voltages across C_1, C_2 at the start of the open-circuit state.

2.3 Parameter Estimation

The Hybrid Pulse Power Characterization (HPPC) test is commonly used for this purpose. The test is conducted with steps as follows:

1. The battery is first fully charged to 100% *SOC* in ways the manufacturer recommends.
2. After resting for a certain period(e.g. 1 hour), the battery is discharged with a constant current pulse (e.g., $0.5C$) for a short duration (e.g., 10s). The voltage response is recorded.
3. Then discharge the battery to another selected *SOC* point (e.g., 90%).
4. Repeat steps 2 and 3 until the battery reaches a low *SOC* point (e.g., 10%) or the maximum discharge limit the manufacturer specifies.

5. If needed, repeat similar steps for charging pulses.

The resting step between pulses allows the exponential term in equation (8) to decay to zero, so accurate U_{OC} can be obtained.

With HPPC data, the model parameters can be estimated through curve fitting techniques. The process are as follows:

- **Estimate R_0 :** The instantaneous voltage drop at the start of each pulse can be used to estimate the internal resistance R_0 , at which point the capacitive effects are negligible.

$$R_0 = \frac{\Delta U_{instant}}{I_{pulse}} \quad (9)$$

- **Estimate R_1, C_1 and R_2, C_2 :** Solve the polarization equation (3), we can get the polarization voltage response:

$$U_{polar} = IR + (U_{init} - IR)e^{-\frac{t}{RC}} \quad (10)$$

where U_{init} is the voltage at the start of the pulse.

Without loss of generality, let $R_1C_1 \leq R_2C_2$, so that the faster electrochemical polarization are represented by R_1, C_1 and the slower concentration polarization effects are represented by R_2, C_2 . Then substitute them into (2), we have:

$$U_t = U_{OC} - I(R_0 + R_1 + R_2) - (U_{1,init} - IR_1)e^{-\frac{t}{R_1C_1}} - (U_{2,init} - IR_2)e^{-\frac{t}{R_2C_2}} \quad (11)$$

By least squares fitting of (11) to the voltage response data during each pulse, we can estimate the values of R_1, C_1 and R_2, C_2 at different SOC points.

- **Estimate Q_{max} :** The maximum capacity Q_{max} can be estimated by integrating the current over the full discharge cycle:

$$Q_{max} = \int_{t_0}^{t_f} I(t)dt \quad (12)$$

where t_0 and t_f are the start and end times of the discharge cycle.

Most of the time this value is provided by the manufacturer.

We use the Samsung INR21700 30T 3Ah Li-ion Battery Dataset [1] to demonstrate the parameter estimation process. The fitting results are shown as follows:

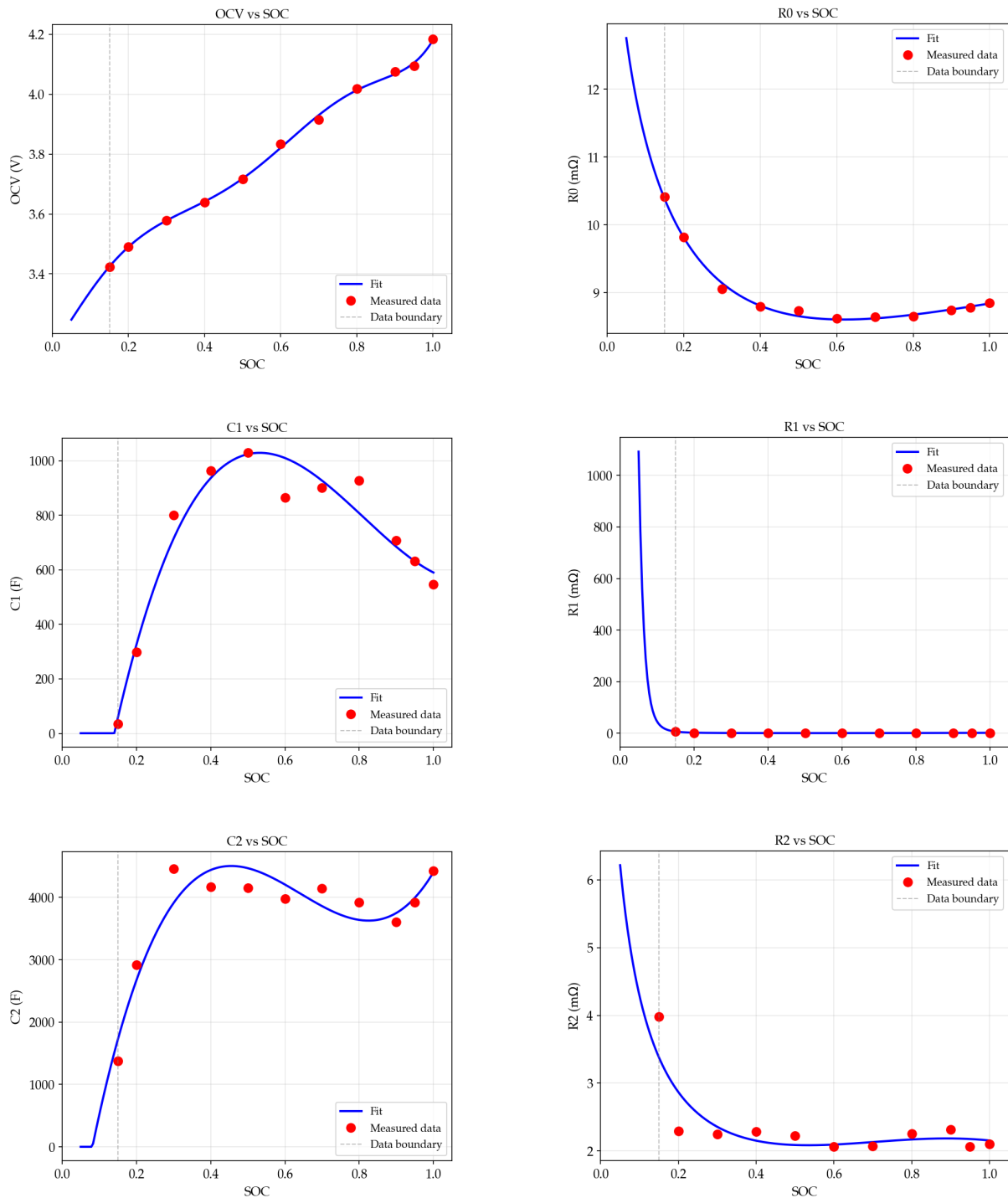


Figure 4: Fitting results of the parameter estimation process.

6-degree polynomial is used to fit the OCV-SOC curve, cubic functions are used to fit the C_1, C_2 , and double exponential functions $y = A_1 e^{B_1 x} + A_2 e^{B_2 x} + C$ are used to fit the R_0, R_1, R_2 curves.

As the fitting result shows, the Ohm resistance R_0 increases significantly when SOC is low, which may be the main reason for voltage drop and device shutdown. Later we will verify this conclusion. Polarization resistances R_1, R_2 also increase when SOC is low, indicating the battery's internal electrochemical processes are hindered. And Polarization capacitances C_1, C_2 decrease when SOC is low, meaning that the battery's ability to respond to load changes is weakened.

Noticed that C_1, C_2 drop to zero when SOC is low, which means the Thevenin model is not valid in that region. However, the smartphone will actually shutdown before the battery reaches such low SOC , because the output voltage will be too low to power the device.

2.4 Simulations

With proper model parameters, we can do numerical simulations of the battery behavior under different load profiles. 2 simplified load profiles are considered here:

- Constant current;
- Constant power.

2.4.1 Constant current

Since the current is constant, equation (4) can be directly integrated to get the SOC at time t :

$$SOC(t) = SOC(0) - \frac{It}{Q_{max}} \quad (13)$$

Then perform Rk45 algorithm to the polarization voltages U_1, U_2 with initial conditions $U_1(0) = U_2(0) = 0$, we can get the final result as follows.

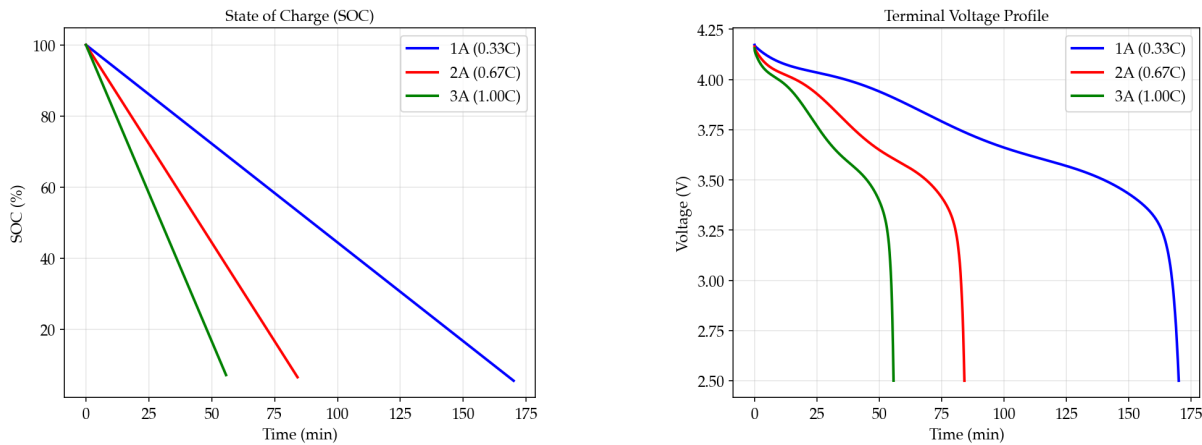


Figure 5: Simulation results under constant current load profile

It can be seen that although the SOC decreases linearly under constant current load, the terminal voltage decreases steadily at first, then suddenly drops to a "dead" value, which makes the device shutdown. The phenomenon is consistent with our daily experience.

2.4.2 Constant power

The output power

$$P = U_t I \quad (14)$$

is constant. In this case, analytic solutions are impossible, so we just use the Rk45 algorithm:

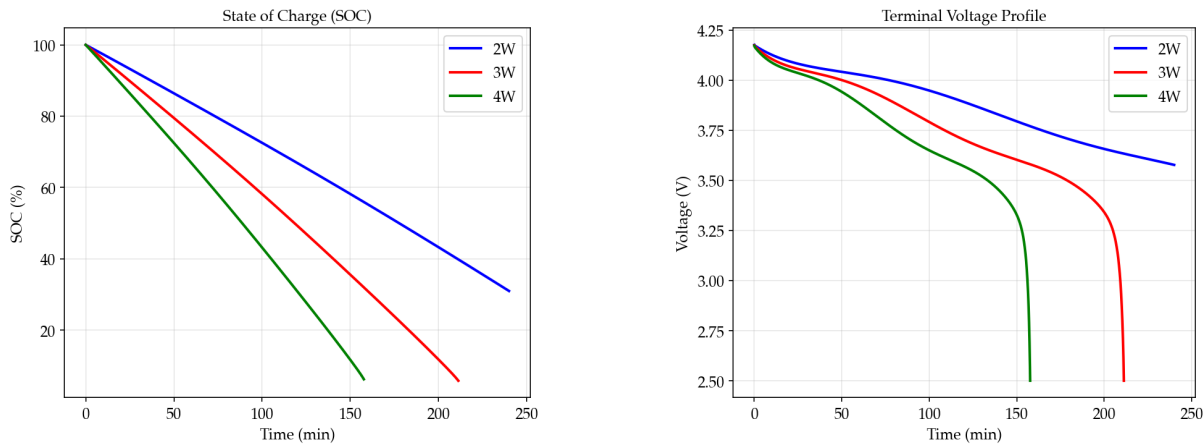


Figure 6: Simulation results under constant power load profile

Similar phenomena can be observed under constant power load profile. However, the terminal voltage drops more rapidly compared to the constant current case, indicating that constant power loads are more stressful to the battery.

3 Actual Battery

3.1 Assumptions

An actual battery is much more complex than the idealized model presented in the previous section. In this section, we will consider more factors that affect the performance and behavior of real batteries:

- **Temperature:** The performance of a battery can vary significantly with temperature. At low temperatures, the internal resistance increases, leading to reduced capacity and power output. Conversely, high temperatures can enhance performance but may also accelerate degradation.
- **Complex Power Profile:** Real batteries often experience varying power demands, which can affect their efficiency and lifespan. High performance demands can lead to increased heat generation, which in turn affects battery temperature.
- **Shutdown Voltage:** Electronics need a minimum voltage to operate correctly. If the battery voltage drops (steadily or suddenly) below this threshold, the device will shutdown even if *SOC* is not zero. In this section, we'll assume that if the battery voltage drops below 3.2V, the device will shutdown immediately.

3.2 Temperature Behavior of Battery

Actual battery behavior is significantly influenced by temperature variations. The most common parameter affected by temperature is the internal resistance. Using the Arrhenius equation, we can model the temperature dependence of internal resistance as follows:

$$R = R_0 \cdot e^{\frac{E_a}{R_u T}} \quad (15)$$

where R_0 is a reference resistance, E_a is the activation energy, R_u is the universal gas constant and T_0 is a reference temperature.

To conduct the regression, rewrite the equation in linear form by taking the natural logarithm:

$$\ln R = \frac{E_a}{R_u} \cdot \frac{1}{T} + \ln R_0 \quad (16)$$

The Samsung INR21700 30T 3Ah Li-ion Battery Dataset [1] contains experimental data at various temperatures. Using this dataset, we perform a linear regression, yielding the following results:

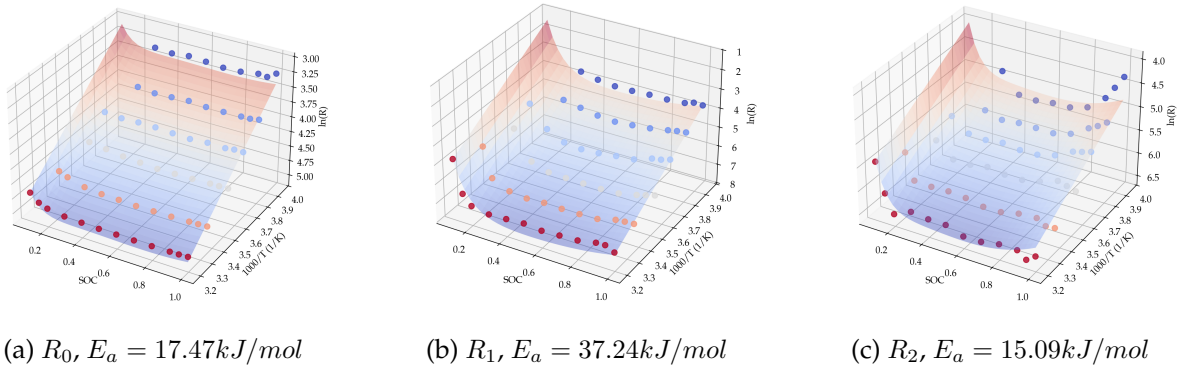


Figure 7: 3D Surface Fitting of Resistance with Temperature and SOC

If we consider the temperature effect, the simulation heatmap of discharge time from 100% SOC under different power load and temperature will be as follows:

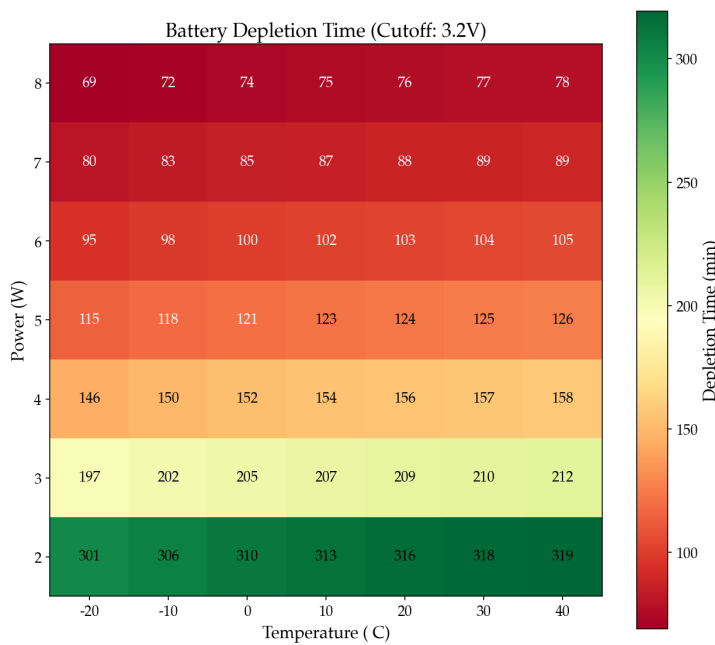


Figure 8: Heatmap of Discharge Time with Power Load and Temperature

It can be observed that battery behaves badly at low temperatures, and the discharge time decreases significantly as temperature drops. However, although high

temperature improves battery short-term performance, it also accelerates battery degradation over time. Therefore, in practical applications, maintaining an optimal temperature range is crucial for battery longevity and performance.

3.3 Battery in Different Work Loads

A smartphone is a complex embedded system whose total power consumption can be decomposed into the sum of contributions from its independent subsystems. According to the **Principle of Power Superposition**, when individual modules share a power supply but operate relatively independently, the total power draw can be expressed as a linear superposition of the power consumption of each module.

Based on a functional module breakdown, we decompose the smartphone's power consumption into the following six primary sources:

- **Display Screen:** Backlight/OLED driver
- **CPU Computation:** Processor dynamic power
- **Network Communication:** WiFi/Cellular radio frequency (RF)
- **Location Service:** GPS reception and computation
- **Audio Playback:** Codec and speaker driver
- **System Mode:** Adjustment effects from power-saving/flight modes

Overall, the model can be written as:

$$P_{total} = P_{screen} + P_{CPU} + P_{network} + P_{GPS} + P_{audio} + P_{mode} \quad (17)$$

By utilizing acquired smartphone state data [3], we estimate the parameters within these models, thereby obtaining a comprehensive power consumption model for complex usage scenarios.

3.3.1 Screen Power

When the screen is on, it exhibits a base power draw plus a near-linear OLED power component (the modeling here assumes an OLED display):

$$P_{screen} = \alpha_S \cdot S + \alpha_B \cdot S \cdot \frac{B}{255} \quad (18)$$

where S is a screen state indicator and B is the brightness level (0–255).

3.3.2 CPU Power

CPU power is the largest variable power source in a smartphone. According to the dynamic power formula for CMOS circuits:

$$P_{dynamic} = C \cdot V^2 \cdot f \quad (19)$$

where C is the load capacitance, V the operating voltage, and f the clock frequency.

Modern processors employ **Dynamic Voltage and Frequency Scaling (DVFS)**, introducing a coupling between voltage and frequency. Empirical studies suggest:

$$V \propto f^{0.5} \Rightarrow P \propto f^{2.5} \quad (20)$$

Furthermore, modern ARM processors commonly adopt a **big.LITTLE heterogeneous architecture**, featuring separate big and small cores with distinct performance and power characteristics. Additionally, actual CPU power depends on its utilization; idle and fully loaded states at the same frequency exhibit significantly different power draws. Thus, we derive the following CPU power model:

$$P_{CPU} = \alpha_U \cdot U + \alpha_{big} \cdot \left(\frac{f_{big}}{f_{max,big}} \right)^{2.5} + \alpha_{small} \cdot \left(\frac{f_{small}}{f_{max,small}} \right)^{2.5} \quad (21)$$

where U represents CPU utilization, and f_{big} , f_{small} are the operating frequencies of the big and small cores, normalized to their respective maximum frequencies.

3.3.3 Network Power

Power consumption in wireless communication stems primarily from the Radio Frequency (RF) front-end, especially the Power Amplifier (PA). According to the Friis transmission equation, received power is inversely proportional to the square of the distance:

$$P_r = P_t \cdot G_t \cdot G_r \cdot \left(\frac{\lambda}{4\pi d} \right)^2 \quad (22)$$

Consequently, to maintain communication quality over distances up to several kilometers for cellular networks, relatively high transmit power is required (typically $200 \sim 500$ mW). In contrast, WiFi communication with a router within tens of meters uses lower transmit power (typically $50 \sim 100$ mW). Moreover, PA efficiency is typically only $30 \sim 40\%$, with substantial energy converted to heat, making network power a significant contributor to total consumption.

Since WiFi and cellular networks are typically used exclusively in practice, our model uses a single indicator variable for network type:

$$P_{network} = \alpha_M \cdot M \quad (23)$$

where M indicates active network type.

3.3.4 GPS Power

The GPS module continuously receives weak signals from multiple satellites and performs complex signal demodulation and position calculation. Its power draw is relatively stable and depends mainly on whether it is active. We adopt a discrete model:

$$P_{GPS} = \alpha_G \cdot G \quad (24)$$

where G is a binary indicator for GPS activity.

3.3.5 Audio Power

The audio module primarily involves compression/decompression processing via an audio DSP, digital-to-analog conversion (DAC), and driving speakers or headphones. We simplify the modeling to a binary indicator for audio playback activity:

$$P_{audio} = \alpha_A \cdot A \quad (25)$$

3.3.6 System Mode Power Adjustment

Modern smartphones offer various system modes for power management, such as Power Saving Mode and Flight Mode. However, most of their energy-saving effects are achieved by altering other parameters (e.g., reducing CPU frequency, limiting network activity), which are already captured by other terms in the model. Therefore, P_{mode} represents additional energy-saving mechanisms. Power Saving Mode may disable unnecessary sensors, reduce refresh rates, and optimize memory management, while Flight Mode directly powers down RF modules. The model is:

$$P_{mode} = \alpha_E \cdot E + \alpha_F \cdot F \quad (26)$$

where E and F are indicators for Power Saving Mode and Flight Mode, respectively. Expectedly, $\alpha_E \leq 0$ and $\alpha_F \leq 0$.

3.3.7 Parameter Estimation and Validation

We performed physically constrained regression using the L-BFGS-B optimizer on normalized and binarized data, enforcing non-negative coefficients for power components and non-positive coefficients for power-saving modes. Substituting the estimated parameters yields the final empirical model:

$$P_{total} = 0.250S + 0.615S\frac{B}{255} + 0.860U + 1.125f_{big}^{2.5} + 0.650f_{small}^{2.5} \\ + 0.696M + 0.040G + 0.397A - 0.068E - 0.028F \quad (27)$$

Subsequently, we can analyze the contribution rate of each parameter and evaluate the model's performance. The following figure illustrates the fitting results and validation:

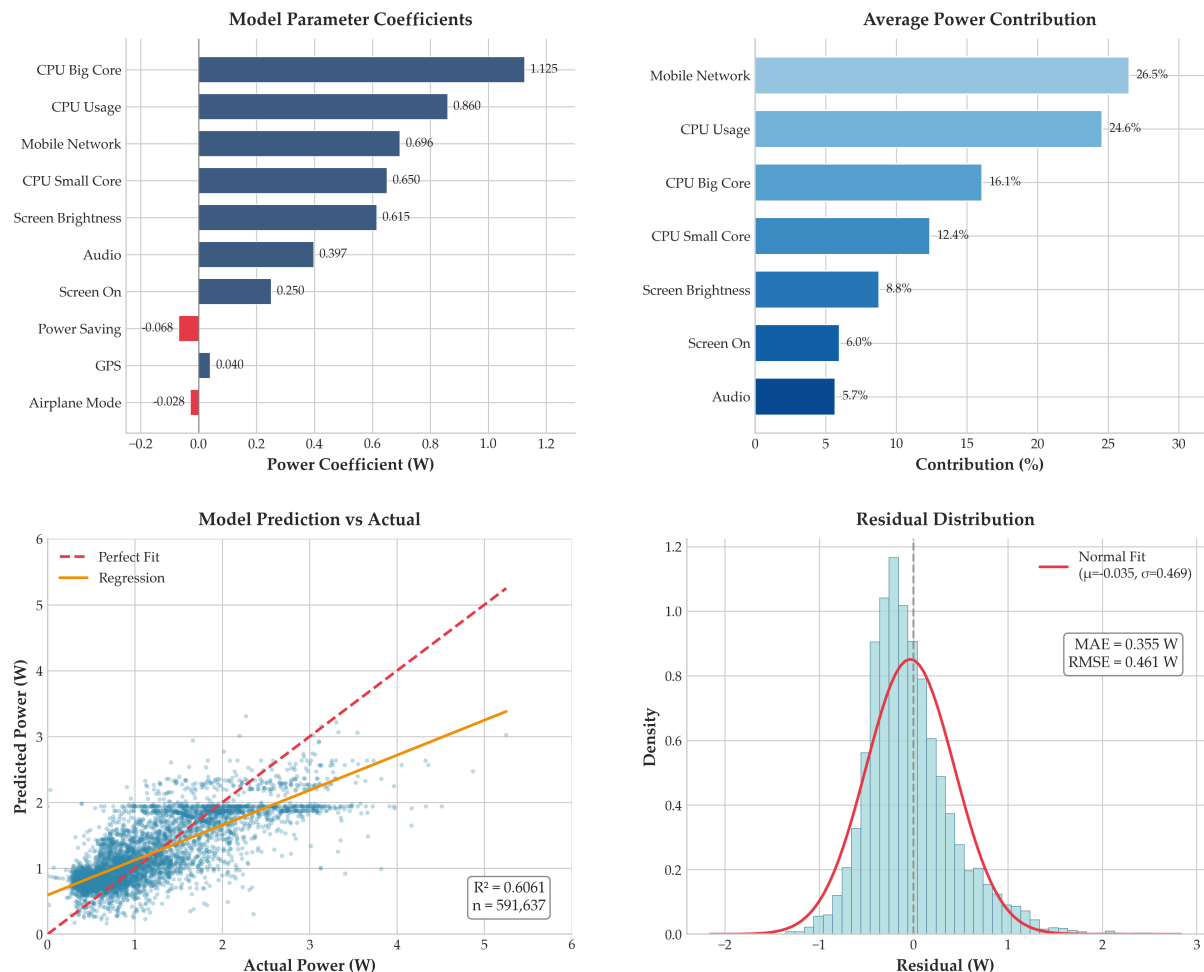


Figure 9: Power consumption model fitting results and validation

Results demonstrate that the white-box power model constructed based on the real-world smartphone dataset achieves satisfactory prediction performance, with an R^2 of 0.606, an MAE of 0.355 W, and an RMSE of 0.461 W. Among the factors analyzed, CPU usage and data network activity exhibit the most significant impact on power draw, whereas GPS consumption and the energy-saving effects of the two included modes show relatively minor influence. As mentioned above, the energy-saving effects of these two modes in practice primarily stem from their influence on the aforementioned features; the small coefficients here reflect that their impact on factors beyond those already captured is relatively minor.

3.3.8 Usage Scenario Simulation

The model allows us to estimate the smartphone's power consumption under various typical usage scenarios. Here are some typical scenarios and their estimated power consumption:

| Scenario | Screen (S) | Brightness (B/255) | CPU Usage | Big Core Freq | Small Core Freq | Mobile Network | GPS | Audio | Total Power (W) |
|-----------------|------------|--------------------|-----------|---------------|-----------------|----------------|-----|-------|-----------------|
| Standby | Off | 0% | 10% | 10% | 10% | No | Off | Off | 0.09 |
| Web Browsing | On | 50% | 50% | 30% | 30% | No | Off | Off | 1.08 |
| Video Streaming | On | 71% | 40% | 40% | 30% | No | Off | On | 1.57 |
| Navigation | On | 100% | 50% | 50% | 40% | Yes | On | On | 2.69 |
| Gaming | On | 100% | 90% | 100% | 100% | Yes | Off | On | 4.51 |

Table 1: Power Consumption Under Different Usage Scenarios

3.4 Heat Transfer Model in High-Performance Scenarios

In this chapter, we discuss how the heat that battery generates affects the temperature of battery itself, and in turn impacts its own performance.

Let Q be the internal heat power, h be the convective heat transfer coefficient, A be the surface area of the battery (assumed to be the area of the smartphone), C be the heat capacity of the battery, T be the battery temperature and T_{env} be the environmental temperature (assumed constant). With Newton's law of cooling, we have:

$$Q = 2Ah(T - T_{env}) + C \frac{dT}{dt} \quad (28)$$

Q can be divided to:

$$Q = Q_{battery} + Q_{processor} + Q_{other} \quad (29)$$

$Q_{battery}$ can be further expressed with the Joule's law:

$$Q_{battery} = I^2 R_{inter} = I^2(R_0 + R_1 + R_2) \quad (30)$$

$Q_{processor}$ often is the major part of heat generation, because processors are often energy-intensive and almost all consumed energy is converted to heat. Here we model $Q_{processor}$ as a part of total power consumption of the device:

$$Q_{processor} = \eta P_{total} \quad (31)$$

in which η is some coefficient.

And the other components' heat generation Q_{other} can be assumed to be a constant for simplicity.

Considering that I and R is time-dependent, equation (28) is a first-order linear ODE. The solution is:

$$T = T_{env} + \frac{1}{C} \int_0^t e^{-\frac{2Ah(t-s)}{C}} Q(s) ds \quad (32)$$

Substitute equation (32) into the Arrhenius' equation, we can get the relation between internal resistance and time, and thus analyze how temperature affects battery performance over time in high-performance scenarios.

The simulation here shows the heatmap of discharge time and max temperature under different power load and environmental temperature. It assumes if the battery

temperature exceeds 50°C , the device will shutdown to protect the battery. In reality, smartphones often decreases processor frequency to reduce heat generation when temperature is too high, but for simplicity we assume an immediate shutdown here.

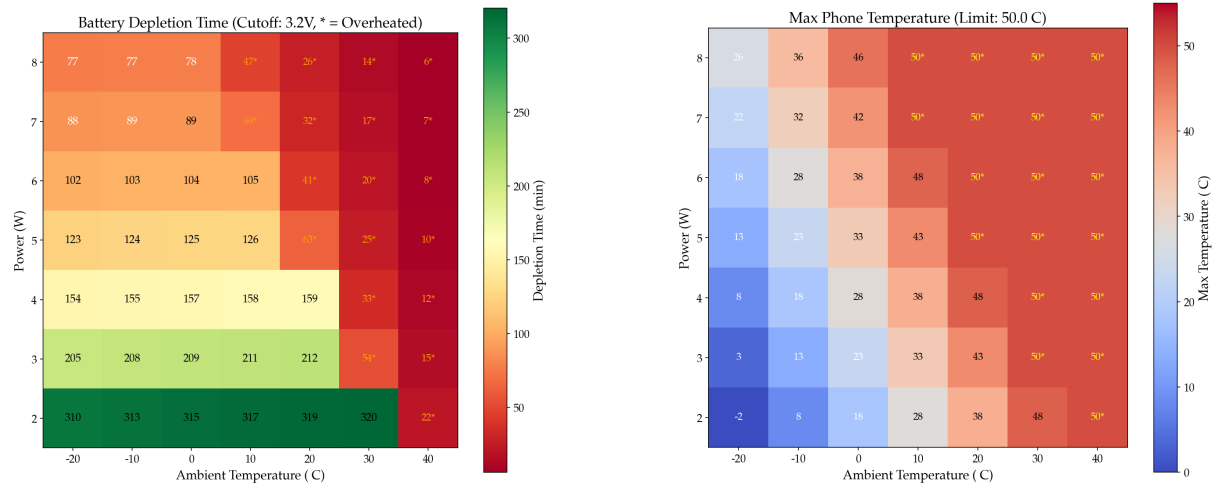


Figure 10: Heatmap of Discharge Time and Max Temperature

In the simulation we set $C = 160\text{J/K}$, $A = 200\text{cm}^2$, $h = 5\text{W}/(\text{m}^2 \cdot \text{K})$, $\eta = 0.5$ and $Q_{other} = 0.8\text{W}$.

It can be observed that high temperature scenarios are quite dangerous for battery operation. Heavy work loads in 30°C or higher can easily lead to battery overheating.

4 Sensitivity Analysis

Smartphone batteries varies in capacity, voltage, and internal resistance. To understand how these variations affect the performance of the system, we conducted a sensitivity analysis by varying each parameter in equation (5) within realistic ranges.

4.1 Time-Varying Properties

Too much simplification leads to lose of actual behavior. For example, setting R_0, R_1, R_2, C_1, C_2 to constants rather than parameters varies with SOC can result in inaccurate predictions. Here is the error result if we simply set them as sample mean values:

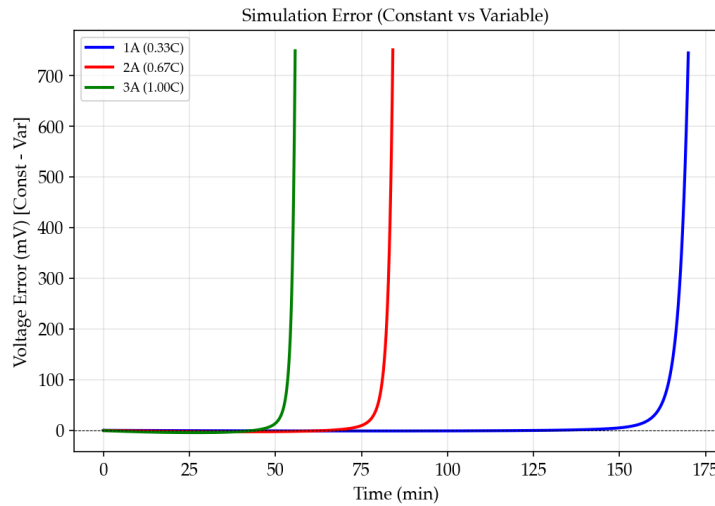


Figure 11: Prediction Error with Constant Electrical Parameters

As shown in Figure 11, the prediction error when SOC is low, which means the behavior that battery resistance increases with lower SOC , is not captured well. This indicates the importance of considering time-varying parameters in battery modeling for accurate predictions.

4.2 Numerical Accuracy

The calibration of electrical parameters of lithium batteries is crucial for accurate modeling and simulation. To assess the impact of numerical accuracy on the calibration results, we add 5%, 10%, 20% disturbance separately to the electrical parameters R_0 , R_1 , R_2 and observe the resulting prediction errors in 1A constant current scenario. The results are shown below:

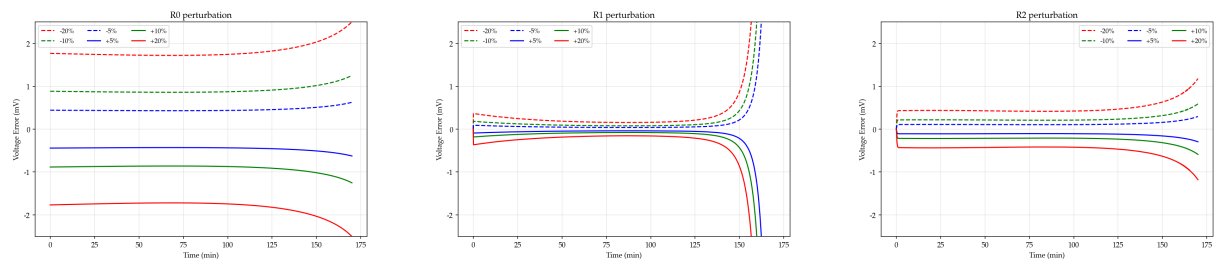


Figure 12: Sensitivity Analysis to Resistance

It can be observed that:

- All of the disturbances lead to prediction errors when SOC is low. Considering the fact that battery resistance increases with lower SOC , The proportional disturbance itself is scaled up, which leads to larger errors.
- The disturbance on R_0 leads to the most significant prediction error, and it is almost independent of time. R_0 is the basic internal resistance. It is not connected to any capacitors, so in constant current scenario, it only affects output voltage.
- The disturbances on R_1 and R_2 have similar sharp pattern at the start. This is because they are connected to capacitors, which cause transient response at the beginning of discharge.

- The errors caused by R_1 are obviously more time-dependent than those caused by R_2 . This is because R_1 is associated with C_1 , which has a smaller time constant, leading to faster transient response. However, this doesn't mean R_2 is less important, as it affects the short-term behavior of the battery during transient events discussing later.

The capacitance effect is not significant in constant current scenario. To further analyze the impact of numerical accuracy on C_1, C_2 , we set a pulse current discharge scenario (1A, 10s, SOC = 80%) to simulate the battery behavior. The results are shown below:

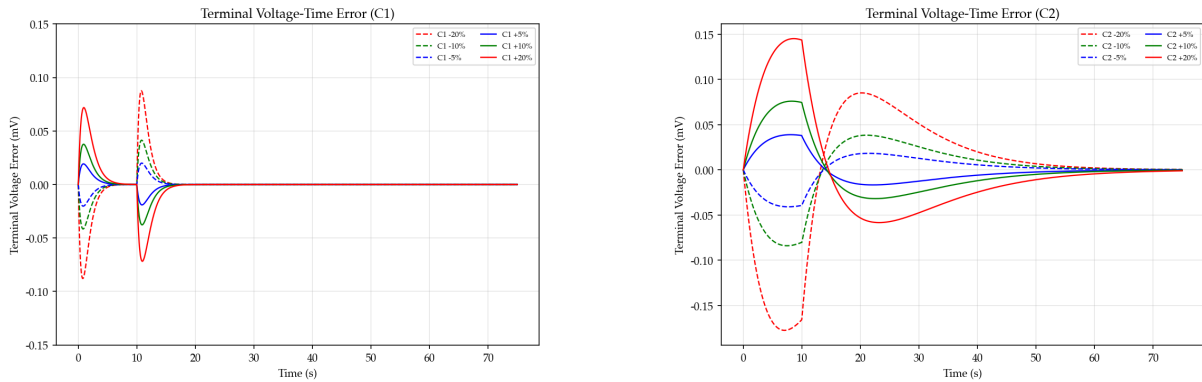


Figure 13: Sensitivity Analysis to Capacitance

It can be observed that the effect of C_1 is faster than that of C_2 , which is consistent with our previous assumptions.

Let $\tau = RC$ is the time constant of the RC circuit that describes how faster an RC circuit responds. When SOC = 80%, we have $\tau_1 = 0.96\text{s}$ and $\tau_2 = 8.84\text{s}$. Therefore, during the 10s discharge pulse, C_1 will have a more immediate effect on the voltage response compared to C_2 , but over a longer period, C_2 will also significantly influence the voltage recovery after the pulse ends. Therefore, both capacitances play important roles in capturing the transient behavior of the battery under pulse discharge conditions, which supports our use of 2-order Thevenin model.

5 User Recommendations

Based on the power consumption model and battery degradation analysis, we provide practical recommendations for smartphone users. These recommendations are organized into two categories: **short-term advice** for extending single-charge runtime, and **long-term advice** for maximizing battery lifespan.

5.1 Short-Term Recommendations: Extending Battery Runtime

For users concerned with maximizing daily battery life, we quantify the effect of various power-saving measures based on our power consumption model. Assuming a constant power draw P , the simplified runtime can be expressed as:

$$T_{\text{runtime}} = \frac{E_{\text{capacity}}}{P_{\text{total}}} \quad (33)$$

where $E_{\text{capacity}} = 15.2 \text{ Wh}$ for our reference 4000 mAh battery.

Using the power model coefficients from Section 3.3, we calculate the battery life improvement for each power-saving action relative to a web browsing baseline (1.08 W). The results are shown in Figure 14.

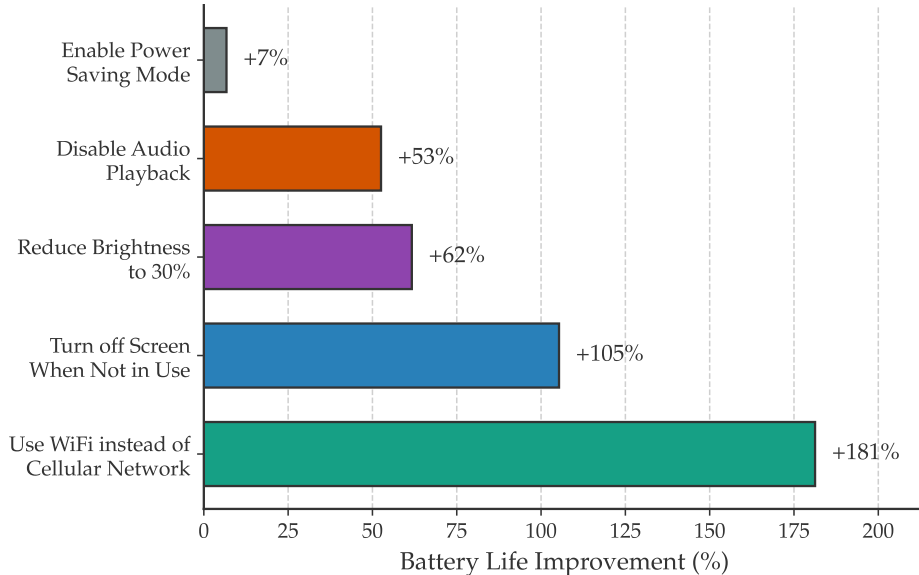


Figure 14: Effect of power-saving measures on battery runtime

Based on these results, we briefly summarize the power-saving actions:

- **WiFi vs. Cellular:** Switching from cellular to WiFi reduces power by 0.696 W, improving battery life by 181%.
- **Screen Off:** Turning off the display when not in use saves approximately 0.554 W (at 50% brightness), extending runtime by 105%.
- **Lower Brightness:** Reducing screen brightness from 100% to 30% saves 0.412 W, a 62% improvement.
- **Disable Audio:** Muting audio playback reduces power by 0.397 W, adding 53% to battery life.
- **Power-Saving Mode:** While providing only +7% direct improvement, this mode is often the simplest solution as it automatically applies multiple optimizations above—reducing brightness, limiting background activity, and restricting network usage.

5.2 Long-Term Recommendations: Maximizing Battery Lifespan

Battery capacity degrades over charge-discharge cycles [5]. We adopt a simplified linear aging model:

$$Q(n) = Q_0 \cdot (1 - \alpha \cdot n) \quad (34)$$

where n is the number of full equivalent cycles and α is the capacity fade rate per cycle.

Using the NASA Li-ion Battery Aging Dataset [4], we fitted $\alpha = 0.000411$ per cycle ($R^2 = 0.97$), indicating 0.041% capacity loss per cycle. At 500 cycles, capacity retention is approximately 79.5%, consistent with the industry standard of 80% end-of-life threshold.

Figure 15 shows the time required for different user types to reach various capacity thresholds, based on their daily energy consumption patterns.

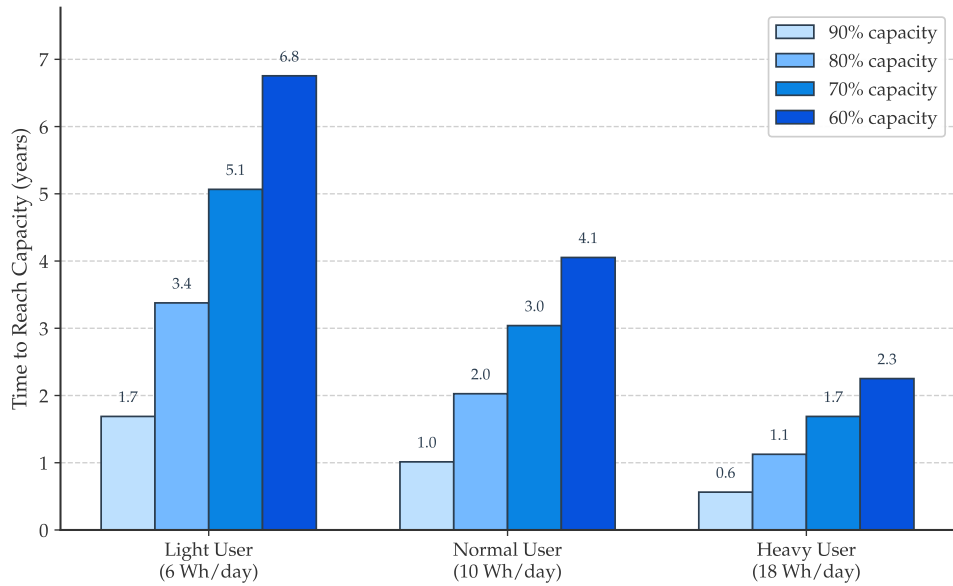


Figure 15: Time to reach different capacity thresholds

Light users (6 Wh/day) can maintain 80% capacity for 3.4 years, comfortably exceeding typical 2-year warranty periods. Normal users (10 Wh/day) reach the 80% threshold at approximately 2.0 years—right at the warranty boundary. Heavy users (18 Wh/day) may need battery replacement within 1.1 years to maintain 80% capacity.

To maximize long-term battery health, we recommend:

- **Reduce daily energy consumption:** Following the short-term recommendations above reduces cycle frequency and extends lifespan proportionally.
- **Maintain 20%–80% charge range:** Avoiding extreme charge states reduces electrochemical stress on the battery.
- **Avoid high-temperature charging:** Elevated temperatures accelerate degradation according to Arrhenius kinetics; remove phone cases during charging.
- **Use standard-speed charging:** Fast charging generates more heat; reserve it for emergencies.

By combining short-term power management with long-term health practices, users can maintain battery capacity above 80% for 2–3 years under normal usage conditions.

A Notation

The following tables summarize all symbols used in this paper.

Table 2: Battery, Thermal, and Power Parameters

| Parameter | Symbol | Physical Meaning | Unit/Range |
|--------------------------------------|-----------------|--|-----------------------|
| <i>Battery Electrical Parameters</i> | | | |
| State of Charge | SOC | Battery capacity percentage remaining | $0 \sim 1$ |
| Open Circuit Voltage | U_{OC} | Voltage when no current flows | V |
| Terminal Voltage | U_t | Measured voltage at battery terminals | V |
| Discharge Current | I | Current flowing out during discharge | A |
| Maximum Capacity | Q_{max} | Total charge capacity of battery | Ah |
| Ohmic Resistance | R_0 | Ionic and electronic conduction resistance | Ω |
| Polarization Resistance 1 | R_1 | Electrochemical polarization (fast) | Ω |
| Polarization Resistance 2 | R_2 | Concentration polarization (slow) | Ω |
| Polarization Capacitance 1 | C_1 | Capacitance for fast dynamics | F |
| Polarization Capacitance 2 | C_2 | Capacitance for slow dynamics | F |
| Polarization Voltage 1 | U_1 | Voltage across R_1-C_1 branch | V |
| Polarization Voltage 2 | U_2 | Voltage across R_2-C_2 branch | V |
| Time Constant 1 | τ_1 | R_1C_1 , fast response time | s |
| Time Constant 2 | τ_2 | R_2C_2 , slow response time | s |
| <i>Thermal Parameters</i> | | | |
| Activation Energy | E_a | Energy barrier in Arrhenius equation | kJ/mol |
| Universal Gas Constant | R_u | Physical constant (8.314) | J/(mol·K) |
| Battery Temperature | T | Real-time battery temperature | K |
| Environment Temperature | T_{env} | Ambient temperature (constant) | K |
| Maximum Temperature | T_{max} | Peak temperature during operation | K |
| Internal Heat Power | Q | Total heat generation rate | W |
| Battery Joule Heat | $Q_{battery}$ | Heat from internal resistance | W |
| Processor Heat | $Q_{processor}$ | Heat from CPU and circuits | W |
| Other Heat | Q_{other} | Heat from other modules | W |
| Heat Transfer Coefficient | h | Convective heat transfer coefficient | W/(m ² ·K) |
| Surface Area | A | Heat dissipation area of device | m ² |
| Heat Capacity | C | Thermal mass of battery system | J/K |
| Heat Efficiency | η | Fraction of electrical power to heat | – |
| <i>Power Components</i> | | | |
| Total Power | P_{total} | Sum of all power components | W |
| Screen Power | P_{screen} | Display system power consumption | W |
| CPU Power | P_{CPU} | Processor power consumption | W |
| Network Power | $P_{network}$ | Wireless communication power | W |
| GPS Power | P_{GPS} | GPS receiver power consumption | W |
| Audio Power | P_{audio} | Audio playback power consumption | W |
| Mode Adjustment | P_{mode} | Power adjustment from system modes | W |

Table 3: State Variables and Model Coefficients

| Parameter | Symbol | Physical Meaning | Unit/Range |
|---|-----------------------|-----------------------------------|---------------------|
| <i>State Variables</i> | | | |
| Screen State | S | Display on/off indicator | {0, 1} |
| Brightness Level | B | Display brightness value | 0 ~ 255 |
| CPU Utilization | U | Fraction of CPU active time | 0 ~ 1 |
| Big Core Frequency | f_{big} | High-performance core frequency | GHz |
| Small Core Frequency | f_{small} | Efficiency core frequency | GHz |
| Network Type | M | 0: WiFi, 1: Cellular | {0, 1} |
| GPS Activity | G | GPS on/off indicator | {0, 1} |
| Audio Playback | A | Audio active indicator | {0, 1} |
| Power Saving Mode | E | Power saving mode on/off | {0, 1} |
| Flight Mode | F | Flight mode on/off | {0, 1} |
| <i>Model Coefficients ($\alpha_S, \alpha_B, \dots > 0$; $\alpha_E, \alpha_F < 0$)</i> | | | |
| Screen Base Coefficient | α_S | Base power when screen on | W |
| Brightness Coefficient | α_B | Power per brightness unit | W |
| CPU Utilization Coefficient | α_U | Power per unit utilization | W |
| Big Core Coefficient | α_{big} | Big core power at max frequency | W |
| Small Core Coefficient | α_{small} | Small core power at max frequency | W |
| Network Coefficient | α_M | Cellular power vs WiFi baseline | W |
| GPS Coefficient | α_G | GPS active power | W |
| Audio Coefficient | α_A | Audio playback power | W |
| Power Saving Coefficient | α_E | Power reduction (negative) | W |
| Flight Mode Coefficient | α_F | Power reduction (negative) | W |
| <i>Battery Aging</i> | | | |
| Current Capacity | $Q(n)$ | Capacity after n cycles | Ah |
| Initial Capacity | Q_0 | Original battery capacity | Ah |
| Cycle Number | n | Number of full equivalent cycles | - |
| Capacity Fade Rate | α | Capacity loss per cycle | cycle^{-1} |
| <i>Time and Evaluation Metrics</i> | | | |
| Time | t | Elapsed time from start | s |
| Battery Runtime | T_{runtime} | Time until battery depletion | h |
| Energy Capacity | E_{capacity} | Total energy capacity | Wh |
| Coefficient of Determination | R^2 | Variance explained by model | 0 ~ 1 |
| Mean Absolute Error | MAE | Average absolute prediction error | same as y |
| Root Mean Square Error | RMSE | Root of average squared error | same as y |

Notes: MAE = $\frac{1}{n} \sum_{i=1}^n |y_i - \hat{y}_i|$, RMSE = $\sqrt{\frac{1}{n} \sum_{i=1}^n (y_i - \hat{y}_i)^2}$, where y_i and \hat{y}_i denote actual and predicted values.

References

- [1] Kollmeyer, P. (2020). Samsung INR21700 30T 3Ah Li-ion Battery Data [Data set]. Mendeley Data. <https://doi.org/10.17632/9xyvy2njj3.2>
- [2] Ouyang, Q., Chen, J., & Zheng, J. (2023). State of Charge Estimation for Lithium-Ion Battery Based on the Fractional Order Equivalent Circuit Model. *IEEE Access*, 11, 107175–107184. <https://ieeexplore.ieee.org/document/10287336>
- [3] Ferreira, D., Gonçalves, J., Kostakos, V., & Dey, A. K. (2024). Android Phone Usage Dataset: Multi-day, Multi-device Usage Logs [Data set]. Mendeley Data, V6. <https://doi.org/10.17632/bpsrw76hgx.6>
- [4] Saha, B., & Goebel, K. (2007). Li-ion Battery Aging Datasets. NASA Open Data Portal. <https://data.nasa.gov/dataset/li-ion-battery-aging-datasets>
- [5] Barré, A., Deguilhem, B., Grolleau, S., Gérard, M., Suard, F., & Riu, D. (2013). A review on lithium-ion battery ageing mechanisms and estimations for automotive applications. *Journal of Power Sources*, 241, 680–689. <https://doi.org/10.1016/j.jpowsour.2013.05.040>

C Use of AI

This section documents authentic interactions between the team and AI assistant (GitHub Copilot) during the development of this paper. These examples demonstrate responsible AI usage focused on **data analysis**, **result interpretation**, and **document formatting**, while all core modeling work was completed independently by the team.

C.1 Battery Dataset Selection

Question: Using 18650 Data for Smartphone Modeling

We found some 18650 cylindrical cell datasets with complete HPPC test data. Can we use 18650 data directly for smartphone battery modeling?

AI Response

Using 18650 data directly for smartphone modeling is not ideal due to several differences:

- **Form Factor:** 18650 is cylindrical with rigid metal casing, while smartphone batteries are flat pouch cells
- **Internal Resistance:** 18650 cells typically have higher resistance due to smaller electrode surface area
- **Thermal Characteristics:** Metal-cased 18650 cells have better heat dissipation; pouch cells are more thermally sensitive
- **Chemistry:** 18650 often uses NCA/NMC, while smartphones typically use LiCoO₂

These differences would introduce systematic errors. I recommend searching for smartphone-specific battery test data if available.

Team's Contribution: Following this advice, we searched for smartphone-specific datasets and found the Samsung INR21700 30T battery dataset, which includes complete HPPC characterization at multiple temperatures (0°C, 23°C, 45°C). We selected this dataset for our parameter identification.

C.2 Dataset Overview and Statistics

Question: Analyzing Dataset Structure

I have a large smartphone usage dataset. Can you help me analyze the overall data distribution and summarize what features are available?

AI Response

Based on your dataset structure, here's an overview:

- **Total records:** 3.24 million discharge data points
- **Target device:** Device ID ab47b5f5ecded6b8 (largest data volume)
- **After filtering:** 2.96 million valid points (excluding battery > 95%)

- **Sampling result:** 591,637 observations for regression

Key features available: screen state and brightness, CPU utilization and core frequencies, network connection status, GPS/Bluetooth/audio states, and power-saving mode indicators.

Team's Contribution: We designed the complete data processing pipeline, defined filtering criteria based on domain knowledge (excluding high battery levels to avoid trickle charging artifacts), and implemented the feature engineering logic.

C.3 Coefficient Reasonableness Analysis

Question: Validating Model Coefficients

My regression model produced these coefficients: Screen On (0.250W), Big Core (1.125W), Small Core (0.650W), Mobile Network (0.696W), GPS (0.040W), Power Saving (-0.068W). Can you help analyze whether they are physically reasonable?

AI Response

These coefficients appear physically reasonable:

1. **Big Core > Small Core:** Consistent with big.LITTLE architecture where performance cores consume more power than efficiency cores.
2. **Mobile Network is significant:** Cellular RF transmission requires higher power than WiFi due to longer communication distances.
3. **GPS is small:** GPS is primarily a receiver with low power consumption.
4. **Power-saving modes are negative:** The small magnitudes suggest most savings come from reducing other parameters already captured in the model.

Team's Contribution: We derived the model structure from first principles (power superposition, CMOS dynamic power formula, DVFS scaling law). AI assisted in reviewing whether the estimated coefficients align with expected physical behavior.

C.4 Data Sampling Strategy

Question: Efficient Sampling for Large Datasets

I have 3 million data points but need to reduce computational cost. What sampling approach would preserve data quality?

AI Response

For time-series data, use systematic sampling (jump sampling) rather than random sampling:

```
df_sorted = df.sort_values('timestamp')
sample = df_sorted.iloc[::5] # Every 5th point
```

This preserves temporal distribution and maintains representation of different usage patterns.

Team's Contribution: We determined the 1:5 sampling ratio based on computational constraints and validated that model coefficients remain stable across different sampling ratios.

C.5 LaTeX Equation Formatting

Question: Breaking Long Equations

My power model equation is too long and overflows the page margin. How do I split it across lines?

AI Response

Use the `aligned` environment inside `equation`:

```
\boxed{\begin{aligned}
P_{\text{total}} &= 0.250S + 0.615S\frac{B}{255} + \dots \\
&\quad + 0.696M + 0.040G + \dots
\end{aligned}}
```

Team's Contribution: The model equation and all physical terms were derived by the team. AI assisted only with LaTeX syntax.

C.6 LaTeX Table Column Width Adjustment

Question: Uniform Table Column Widths

My notation table has inconsistent column widths, and the table is too narrow compared to the page width. How can I make all columns have uniform width and expand the table to fill the text width?

AI Response

Use the `tabularx` package with equal-width columns:

```
\usepackage{tabularx}
\newcolumntype{Y}{>{\centering\arraybackslash}X}

\begin{tabularx}{\textwidth}{|Y|Y|Y|}
\hline
\textbf{Symbol} & \textbf{Description} & \textbf{Unit} \\
\hline
\$R_0\$ & Ohmic resistance & \$\Omega\$ \\
\hline

```

```
...
\end{tabularx}
```

The X column type automatically distributes remaining width equally. Using \textwidth ensures the table spans the full page width.

Team's Contribution: We created all table content and symbol definitions. AI assisted with LaTeX table formatting syntax.

C.7 Summary of AI Usage

| Category | AI Assistance | Team Responsibility |
|-----------------------|---------------------------------|---------------------------------|
| Core Modeling | — | Thevenin model, Arrhenius, DVFS |
| Data Selection | Advised against 18650 | Found Samsung dataset |
| Data Analysis | Dataset statistics | Filtering, feature engineering |
| Result Interpretation | Coefficient review | Model fitting, validation |
| Documentation | LaTeX table/equation formatting | All technical writing |

Table 4: Division of work between AI assistance and team contribution

C.8 Declaration

All theoretical frameworks in this paper—including the second-order RC equivalent circuit model, Arrhenius temperature dependence, CMOS dynamic power formula ($P \propto f^{2.5}$), Friis transmission equation for RF power, and Newton’s law of cooling for thermal modeling—were **independently researched, derived, and implemented by the team members**. AI tools were used for comparing battery types, understanding dataset structure, reviewing coefficient reasonableness, and LaTeX formatting—reflecting responsible AI assistance for productivity enhancement without replacing human judgment in scientific analysis.